ACS Macro Letters

Letter

pubs.acs.org/macroletters

Internal Correlations and Stability of Polydots, Soft Conjugated Polymeric Nanoparticles

Sabina Maskey,[†] Naresh C. Osti,[†] Dvora Perahia,*[,†] and Gary S. Grest[‡]

[†]Department of Chemistry, Clemson University, Clemson, South Carolina 29634, United States

[‡]Sandia National Laboratories, Albuquerque, New Mexico 87185, United States

Supporting Information

ABSTRACT: Conjugated polymers collapsed into long-lived highly luminescent nanoparticles, or polydots, have opened a new paradigm of tunable organic particles with an immense potential enhancing intracellular imaging and drug delivery. Albeit the chains are not in their equilibrium conformation and are not confined by cross-links, they remain stable over astounding long times. Using fully atomistic molecular dynamics simulations with an innovative method to controllably collapse an inherently rigid polymer, we determined for the first time the internal structure and stability of polydots made of dialkyl-*para*-phenylene ethynylene, immersed in water, a biological relevant medium. In contrast to natural aggregates, the aromatic rings within the polydots are uncorrelated, with little to no water in its interior. This lack of correlation explains the differences of luminescence characteristics between spontaneously aggregated conjugated polymers and polydots. Resolving the conformation and stability of these particles will enable transforming an idea to a new effective tool.

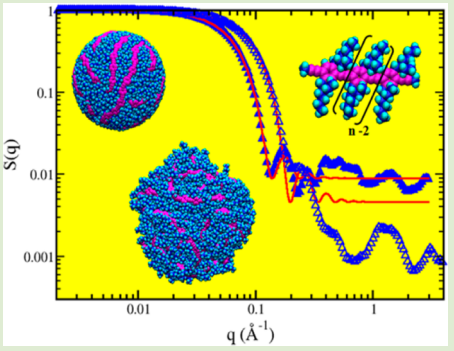

Conjugated polymers collapsed into long-lived, nanometer-size, globular conformations form a new class of light-emitting and absorbing soft particles. Their luminescence characteristics differ significantly from those of spontaneously aggregated conjugated polymers, pointing to a new conformation of the rigid polymers in confined geometry.[1] The chemistry and the softness of these nanoparticles (NPs) present a new tunable manifold that will augment the use of organic NPs at interfaces with biological membranes, as sensors, as imaging markers, and as targeted-drug delivery tools.[1−5] These particles consist of a multitude of chromophores confined into small dimensions, often on the same order of magnitude as the size of biological membranes. They are luminescent, and their surface can be modified to either tether them to an interface or graft functionalities that allow their insertion into living organisms. Packing a large number of chromophores into a small particle while retaining the ability of the molecule to absorb and emit light results in a unique hybrid that combines the advantages of organic dyes and the high brilliance characteristics of inorganic NPs and quantum dots. Therefore, the polydots open a new paradigm, where a single molecule-particle can be detected. Here we probe the internal conformation and the stability of one model polydot which is a critical first step to design soft organic NPs with defined properties, using newly designed computational tools. Beyond the insight into the structure and stability of polydots, the study provides new insight into the behavior of confined polymers.

The majority of conjugated polymers are relatively rigid, and their collapsed state is far from the equilibrium conformation.[6,7] These macromolecules are often forced into the nano-dimension by imposing constraints on the polymer backbone, either cross-linking or physically trapping the chains into a confined space. The most common approach to achieve long-lasting nanoconfigurations is to cross-link the polymers, where the resulting dimensions depend on the molecular weight of the polymer, its smallest rigid segment, and the number of cross-links.[8,9] A new fascinating pathway to form highly luminescent NPs is to confine polymers to a NP without cross-linking.[10] These particles are of particular interest since rearrangements of the chromophores can take place. The conformational freedom of the polymer chains leads to a new class of tunable particles. Their unique photophysics[3,11] is often determined by the conformation of the polymer backbone.

Here we probe the interactions that underlie the formation and internal structure of these long-lived soft NPs formed by physical confinement of the macromolecules using atomistic molecular dynamics (MD) simulations. Computational studies are among the very few methodologies that can directly probe the conformation of the polymer chains and derive the internal correlations *within* a soft NP. The highly congruent experimental and computational structure factors of the shape of the polydot serves as a bridge between macroscopically measured properties and internal structure and correlations within the polydot obtained from computational studies.

Experimentally, these soft NPs are formed by dissolving an aliquot of polymer in a good solvent, below the critical micellar

Received: May 6, 2013
Accepted: July 12, 2013
Published: July 23, 2013

 © 2013 American Chemical Society

concentration.[3,12] The solutions are then dripped into a poor solvent such as water, while vigorously mixed via sonication, forming polymer-containing nanometer size droplets dispersed in the poor solvent.[3,10,12] As the good solvent evaporates, the polymers collapse into NPs that remain suspended in the poor solvent.

The process results in long-lived, luminescent NPs that consist of polymers collapsed into dimensions that are smaller than their inherent rigid segment.[3,10,12] These polymeric NPs, often referred to as polydots, not only remain fluorescent but can be inserted into living organisms.[13−15] The fluorescence characteristics of polydots indicate that the structure of the confined polymer molecules differs from that in melts or in spontaneously formed aggregates. The soft nature of the polydots and their inherently organic exterior enhance the ability to tailor specific chemistries at the polymer interface needed for different functions. Resolving the internal structure and dynamics of these confined polymers is fundamental to the design of polydots with well-defined photophysics.

The current study uses MD simulations to probe directly for the first time the internal structure of long-lived NPs formed by dialkyl-*para*-phenylene ethynylene (PPE). PPEs are hardly soluble in water and assume extended conformation even in good solvents such as toluene and tetrahydrfurane. Experimentally, PPE polydots remain in aqueous solutions without cross-linking for extended periods of time. PPEs are uniquely tunable polymers since the degree of coplanarization of the backbone aromatic rings determines the degree of conjugation and therefore the absorption and emission characteristics. The backbone becomes fully conjugated when all aromatic rings lie in the same plane. The side chains grafted on the backbone impact the solubility and assembly of the PPEs and, indirectly, the electronic structure of the polymer. Overall, the light-emitting and absorption characteristics of PPEs strongly depend on the chemical structure of the backbone and the side chains that together determine the conformation of the polymer.[7,16]

Using a process close to the experimental preparation method, we were successful in computationally forming polydots that consist of PPEs. The NPs were formed by compressing an isolated chain in an implicit poor solvent. The molecules were enclosed in a large spherical cavity, the radius of which was slowly reduced over 1 ns. The cavity wall interacted with the PPE chain via a harmonic potential.[17] The encapsulation within a spherical cavity provides a parallel to the experimental process in which the polymers are trapped in droplets of good solvents that are immersed in a poor solvent. As the good solvent evaporates experimentally the polymer cage becomes smaller, mimicked here by decreasing the size of the confining cavity. PPE with a polymerization number of 240 with disubstituted by ethyl hexyl side chains, as prepared and in its early stages of compression, is shown in Figure 1a and b. The polymer molecules were initially compressed to dimensions that result in internal density comparable to that of the polymer melt. This criterion resulted in a final diameter of 5.0 nm for a diethyl-hexyl PPE and 2.0 nm for a PPE without side chains. Once the melt density reached bulk value, the spherical cavity was removed, equivalent to the experimental stage where all of the good solvent evaporated, and the polydots were placed in implicit solvents to equilibrate.

A snapshot of the diethyl-hexyl PPE polydot as prepared is shown in Figure 1c. Following the release of the cavity, the polydot assumed a fully spherical shape with a smooth interface

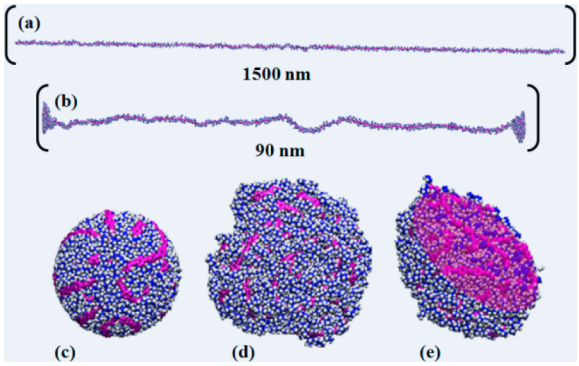

Figure 1. Snapshots of diethylhexyl PPE of polymerization number 240, for (a) t = 0 ns, (b) t = 0.5 ns, and (c) t = 1 ns in an implicit poor solvent. The final diameter of the indenter is 5.0 nm. (d) Polydot in water after 25 ns and (e) a slice through the center of the polydot presented in d. For clarity, dark blue corresponds to carbon atoms on side chains; hydrogen atoms on side chains are white, and the backbone is represented by magenta. Separate visualizations of the backbone and the side chains in water and implicit solvents are given in the Supporting Information, Figure S1.

dominated by the side chains. Following a short equilibration in an implicit poor solvent the collapsed polydots were relaxed in solvents of varying quality, including water and toluene, as well as in good and poor implicit solvents.

The stability of the polydot strongly depends on the solvent quality, as one would expect for a collapsed polymer that is not cross-linked. When placed in water, the polydots slightly changed their conformation, as shown in Figure 1d, but remained in their nanoconfiguration for up to 25 ns in water and 100 ns in explicit a poor solvent. Water is a poor solvent for PPEs; however, the small number of molecules that do dissolve remain extended or aggregated, rather than collapsed. This stability over extended periods is consistent with experimental observations where the polydots remain stable over months in their collapsed state, dispersed in water. In comparison with neutron spin echo results, these computational intervals are sufficient for most local dynamics to take place. A first insight into the structure of the polydot can be obtained by slicing it through its center, as shown in Figure 1e. The center of the polydot is dense, and no obvious spatial correlations were observed and no water molecules.

In contrast to the conformation of the polydot in water, in toluene, the chain rapidly unfolded. Snapshots of diethyl hexyl PPE polydots in toluene at times ranging from 5 to 100 ns after the indenter was removed are presented in Figure 2. To probe a longer time scale, implicit poor and good solvents are used.[6] We found that the results for an implicit poor solvent are

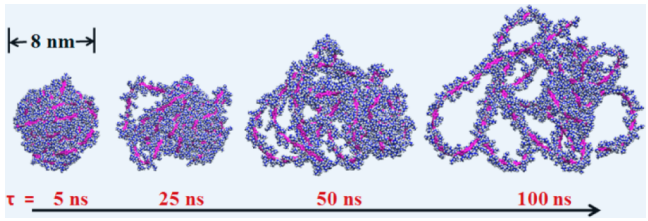

Figure 2. Time sequence for polydots that consist of diethyl ethyl PPE in toluene. Carbon atoms on side chain are marked in dark blue, hydrogen on side chain in white, and backbone is represented by magenta.

dx.doi.org/10.1021/mz400225d | *ACS Macro Lett.* 2013, 2, 700−704

similar to those obtained for water. The results for polydots in an implicit good solvent are similar to those obtained for toluene, while reflecting the fact that the backbone and the side chains interacted equally with the solvent, whereas toluene is a better solvent for the backbone than for the side chains of the PPE. The implicit solvents will be referred in the rest of the paper as poor and good.

The dimensions of the polymers in toluene are smaller than the dimensions of those in a good implicit solvent for the same unraveling time. These differences present a remarkable demonstration of the significance of specific interactions of the segments of polymers with solvents. In an implicit good solvent, the interactions of the backbone and the side chains with the solvent are equally good, whereas the interactions of toluene with the backbone and side chains are different. In contrast, the dimensions of the polydots in both water, which is a poor solvent for both the backbone and the side chains, and in an implicit poor solvent, are similar.

The radius of gyration of the polymer was measured as a function of time after the polydots were immersed in the four solvents. Figure 3 presents R_g as a function of time for PPE

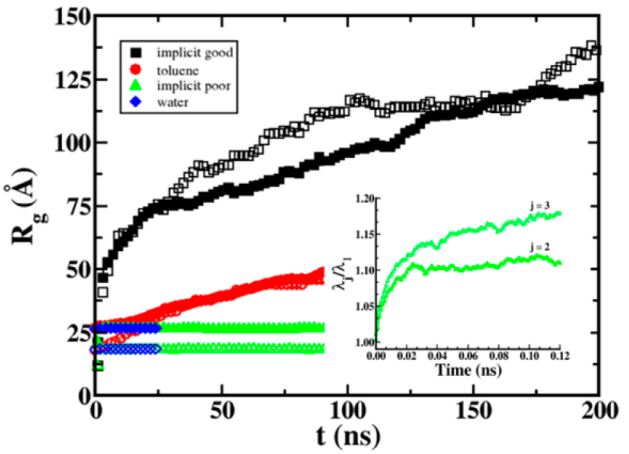

Figure 3. Radius of gyration R_g of the PPE molecule as a function of time in water and toluene, poor and good solvents for substituted PPE (solid symbols) and without side chains (open symbols). The inset presents the ratios for the moment of inertia for an implicit poor solvent for first 0.12 ns.

polydots with and without side chains. After a very small expansion of the polydot in the first few picoseconds after the indenter was removed, the polydots remained collapsed for the length of the simulation in both water and the implicit poor solvent.

Surprisingly, the presence of alkyl side chains did not enhance the stability of the polydot in poor solvents. This observation suggests that the stability is achieved through arrest of the backbone motion at temperatures below the glass transition of the polymer rather than interdigitation of the side chains. In the two good solvents, however, R_g of the polydot continued to increase over the course of the simulation as the chain unraveled. After an initial faster increase in R_g in the good solvent compared to toluene, the rate of increase in R_g was comparable for the two solvents for late times. From these results, it is clear that the conformational stability of the polydot depends strongly on the solvent−polymer interactions.

In contrast to having little or no effect on the stability of the NPs in poor solvents, the lack of side chains enhanced the rate of unraveling of the polymer in good solvent, as shown in Figure 3. Though the polydots were locked into place by the backbone in the poor solvents, their packing was impacted by the side chains. As the backbone becomes dynamic, the side chains affected the conformational dynamics of the polymer.

The evolution of the shape of the polydots was probed by calculating the three eigenvalues of the moment of inertia tensor λ_1, λ_2, and λ_3. The ratios of the two largest eigenvalues to the smallest one, immediately following the release of the constraints for implicit poor solvent, are shown in the inset of Figure 3. The ratio of the eigenvalues which is one at the onset as expected for a fully spherical particle[18] increases with time for the first 20 ns and then fluctuates around $\lambda_3/\lambda_1 = 1.2$ and $\lambda_3/\lambda = 1.1$. For PPEs with no side chains, $\lambda_3/\lambda_1 = 1.6$ and $\lambda_2/\lambda_1 = 1.2$. These eigenvalues show that the PPEs with side chains are significantly more spherical than those made of bare PPEs. This is the first observation that the side chains impact the packing of the backbone. The ability of the polymer to rearrange following the removal of the constraint shows that the preparation method does not lock the polymer conformation.

The radial density of the polydots from their center of mass is shown in Figure 4 in water and in a poor solvent. The density

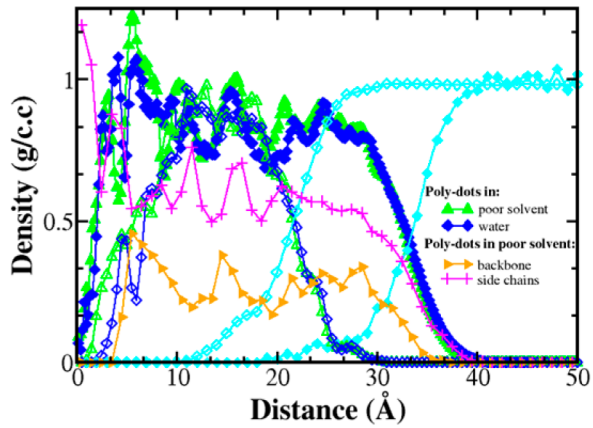

Figure 4. Radial mass density of the polymer and water within polydots. Zero corresponds to the center of the particle. The solid symbols correspond to substituted PPEs and open symbols to PPEs without side chains. The PPE in water is represented by diamonds and in poor solvent by circles. The density profiles of water are marked by triangles.

of the polydot with side chains is uniform, within the noise of the measurement, while the density for the polydot without side chains is lower near the center. Little or no water molecules are found inside the polydot in both cases; however at the boundary between the outer surfaces of the polydots a higher density of water is observed over a range of approximately 1 nm. The access is in part due to the fact that the polydots are not perfectly spherical, and their external interface is rough, particularly those without side chains. Comparing the density of the side chains and the backbone separately, the side chains dominate the surface of the polydots. Undulations observed may correspond to the dimensions of a tube that encapsulate the backbone and side chains.

An important aspect of the functionality of polydots for light absorption and emission is the correlation between the aromatic rings. One measure of the correlation of the aromatic rings within the PPE backbone was obtained using a first-order

dx.doi.org/10.1021/mz400225d | ACS Macro Lett. 2013, 2, 700−704

orientation order parameter, given by $P_\theta = 1/2\ \langle 3(\cos^2\theta) - 1\rangle$, where P_θ corresponds to the average alignment of aromatic rings with a particular spatial direction, and θ is the measure of deviation perpendicular to the interface for two aromatic rings which are separated along the backbone by a degree of polymerization Δn. P_θ has a range of $[-1/2, 1]$.[19] Results for P_θ for polydots with and without side chains in water are shown in Figure 5. In agreement with our previous results for extended

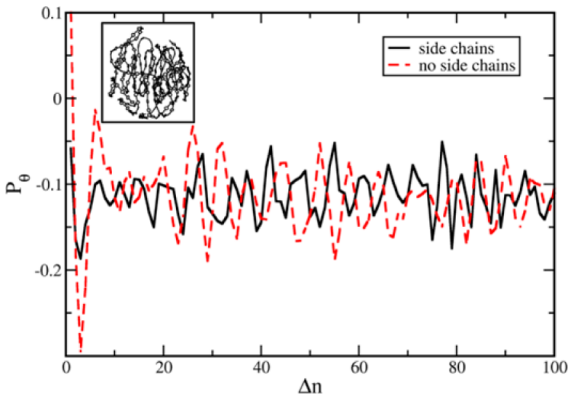

Figure 5. Order parameter P_θ as a function of the separation of phenyl rings Δn in the aromatic plane for polydots substituted (solid black line) and without (dashed red line) side chains in water. Insert shows the snapshot of the polydot with side chains in which only the backbone carbon atoms are shown and side chains and hydrogen atoms are removed for clarity. Data are averaged over 200 configurations.

PPE chains, no correlations were observed between the orientations of the aromatic rings beyond the error in the estimate of P_θ, except for the nearest neighbor ring, which have a tendency to align perpendicularly. This lack of correlation between the aromatic rings accounts for their light emission and absorption characteristics.

The calculations of the correlations within the polydots have provided the first insight into their luminescence behavior. In order to bridge between structural experimental studies and computational ones we calculated the structure factor $S(q)$, where q is the momentum transfer vector. $S(q)$ is the most accurate experimental measure of the structure of polydots. The analysis of the experimental scattering data is often model-dependent and requires further support. The scattering factor of the polydots was calculated using: $S(q) = |\sum_i b_i e^{iqr_i}|^2$ where b_i and r_i are the scattering length and position vector of atom i, respectively.[20] The results for the calculated $S(q)$ of the polydots in water are shown in Figure 6. These simulation results capture the shape of the NPs in the low q region together with internal structural features at high q.

The calculated $S(q)$ was modeled with a typical sphere scattering convoluted with a Gaussian to describe a gradual drop-off in the scattering length density.[21] The results are shown in Figure 6. This fitting resulted in a radius of gyration of 25.1 Å for the PPE with side chains and 17.6 Å without side chains. These compare to the values of $\langle R_g^2\rangle^{1/2}$ = 26.8 Å for PPE with side chains and 18.2 Å without side chains determined directly. The results obtained by simulations are similar to those obtained separately (not shown) by neuron scattering. This multiple length scale insight into the structure of the polydot is unique to computational studies and cannot be captured experimentally.

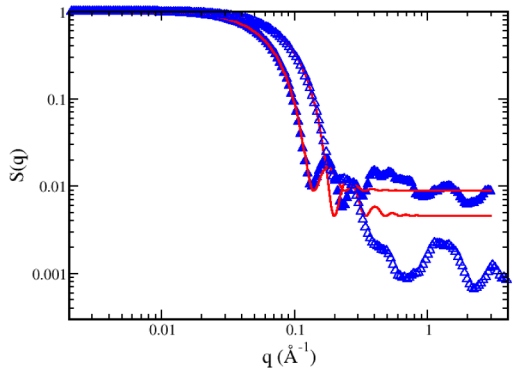

Figure 6. $S(q)$ as the function of q for polydots substituted (solid triangles) and without (open triangles) side chains in water. The best fit to a fuzzy spherical form factor[21] is shown by solid lines.

In conclusion, this study introduces the first insight into the structure of a new type of luminescent particles that consist of conjugated polymers collapsed into the nanodimension, as obtained from MD simulations. The simulations conceptually mimic the experimental caging of the polymer within boundaries of a droplet to force a collapsed geometry. A spherical smooth NP with the alkyl chain dominating the surface of their interface was formed. The NPs were placed in four different solvents, and their structure was followed as a function of time. In water and poor solvent, the polydots remained predominantly spherical and compact, while their interface became significantly rough. In toluene as well as in a good solvent, the polymer unraveled as a function of time. The alkyl side chains affected the symmetry of the NP in water, where the alkyl-substituted polymer forms a more spherical NP, but no effect was observed for the stability of the polydot. This suggests that the frozen conformation of the polymer below the glass transition temperature is the prime factor that retains the stability of the polydots in poor solvents. No internal correlations were observed between the aromatic rings on the polymer within the polydot, consistent with the experimental luminescence of PPEs. This study has opened the way to explore internal structures of soft nanoparticles that in turn will impact the design of new NPs with well-defined luminescent characteristics.

■ ASSOCIATED CONTENT

Ⓢ Supporting Information

Model and methodology details. This material is available free of charge via the Internet at http://pubs.acs.org.

■ AUTHOR INFORMATION

Corresponding Author

*E-mail: dperahi@clemson.edu.

Notes

The authors declare no competing financial interest.

■ ACKNOWLEDGMENTS

The authors gratefully acknowledge financial support from DOE Grant No. DE-FG02-12ER46843. This work was made possible by advanced computational resources deployed and maintained by Clemson Computing and Information Technology. This work was performed, in part, at the Center for Integrated Nanotechnology, a U.S. Department of Energy and Office of Basic Energy Sciences user facility. Sandia National

Laboratories is a multi-program laboratory managed and operated by Sandia Corporation, a wholly owned subsidiary of Lockheed Martin Corporation, for the U.S. Department of Energy's National Nuclear Security Administration under Contract No. DE-AC04-94AL85000. We thank S. J. Plimpton, F. Pierce, and J. McNeill for helpful discussions.

REFERENCES

(1) Tuncel, D.; Demir, H. V. *Nanoscale* **2010**, *2*, 484−494.
(2) Pecher, S.; Mecking, S. *Chem. Rev.* **2010**, *110*, 6260−6279.
(3) Wu, C.; Chiu, D. T. *Angew. Chem., Int. Ed.* **2013**, *52*, 3086−3109.
(4) Dorresteijn, R.; Haschick, R.; Klapper, M.; Müllen, K. *Macromol. Chem. Phys.* **2012**, *213*, 1996−2002.
(5) Cordovilla, C.; Swager, T. M. *J. Am. Chem. Soc.* **2012**, *134*, 6932−6935.
(6) Maskey, S.; Pierce, F.; Perahia, D.; Grest, G. S. *J. Chem. Phys.* **2011**, *134*, 244906.
(7) Perahia, D.; Traiphol, R.; Bunz, U. H. F. *Macromolecules* **2001**, *34*, 151−155.
(8) Beck, J. B.; Killops, K. L.; Kang, T.; Sivanandan, K.; Bayles, A.; Mackay, M. E.; Wooley, K. L.; Hawker, C. J. *Macromolecules* **2009**, *42*, 5629−5635.
(9) Liu, J. W.; Mackay, M. E.; Duxbury, P. M. *Europhys. Lett.* **2008**, *84*, 46001.
(10) Szymanski, C.; Wu, C. F.; Hooper, J.; Salazar, M. A.; Perdomo, A.; Dukes, A.; McNeill, J. *J. Chem. Phys. B* **2005**, *109*, 8543−8546.
(11) Yu, J.; Wu, C.; Tian, Z.; McNeill, J. *Nano Lett.* **2012**, *12*, 1300−1306.
(12) Wu, C.; Szymanski, C.; McNeill, J. *Langmuir* **2006**, *22*, 2956−2960.
(13) Wu, C. F.; Bull, B.; Szymanski, C.; Christensen, K.; McNeill, J. *ACS Nano* **2008**, *2*, 2415−2423.
(14) Li, K.; Liu, B. *J. Mater. Chem.* **2012**, *22*, 1257−1264.
(15) Howes, P.; Green, M.; Levitt, J.; Suhling, K.; Hughes, M. *J. Am. Chem. Soc.* **2010**, *132*, 3989−3996.
(16) Halkyard, C. E.; Rampey, M. E.; Kloppenburg, L.; Studer-Martinez, S. L.; Bunz, U. H. F. *Macromolecules* **1998**, *31*, 8655−8659.
(17) Plimpton, S. *J. Comp. Phys.* **1995**, *117*, 1−19.
(18) Theodorou, D.; Suter, U. W. *Macromolecules* **1985**, *18*, 1206−1214.
(19) Hariharan, A.; Harris, H. J. *J. Chem. Phys.* **1994**, *101*, 4156−4165.
(20) Sorensen, C. M. *Aerosol Sci. Technol.* **2001**, *35*, 648−687.
(21) Stieger, M.; Richtering, W.; Pedersen, J. S.; Lindner, P. *J. Chem. Phys.* **2004**, *120*, 6197.